Comparison of approaches to landmark identification on 3D torso surface meshes for breast reconstruction

S. Foster, P.J. Morrow, B.W. Scotney, R.J. Winder, S.A. McIntosh

Faculty of Computing & Engineering,
Coleraine Campus, Ulster University

Belfast Health and Social Care Trust

Abstract

Breast reconstruction is a vital part of breast cancer treatment for many women and can contribute to maximizing their quality of life by reducing the impact of breast cancer on their physical appearance. The limited reproducibility of subjective outcome evaluation techniques including panel evaluation has indicated a need for objective methods. Anthropometry requires fiducial points to be directly marked on the torso of subjects being assessed or indirectly on photographs before measurements are carried out, however subjectivity still exists with anthropomorphic techniques. Automating the identification of fiducial points such as the nipples will permit more consistent and reproducible quantitative measures of breast morphology. This paper investigates algorithms for automatic detection of nipples on 3D surface images and the impact that applying various thresholding and clustering operations on 2D texture data has on the automated placement of the nipple compared to the ground truth manually marked location.

Keywords: Image Processing, landmark detection, 3D surface mesh, segmentation, objective evaluation

1 Introduction

During 2010-2014 in Northern Ireland, 1,283 females were diagnosed with breast cancer per year and 306 per year died from the disease, with the lifetime risk of women developing breast cancer being 1 in 11 [1]. In the last 10 years female death rates have fallen by around a fifth [2], which may be due to earlier diagnosis through the introduction of breast cancer screening and advancements in treatments including chemotherapy, radiotherapy and surgery. Breast cancer surgery may involve partial removal of the breast or a mastectomy procedure during which the entire breast is removed. Breast reconstruction is the rebuilding of the breast mound using prosthetic implants or tissue taken from other parts of the body to create a natural breast shape [3]. Sabczynski *et* al. [4] developed a system to support surgeons in surgical planning by permitting visualization of the foreseen breast surgery results, this provides patients with opportunity to participate in a Shared Decision making process with their clinicians.

Evaluating the cosmetic outcome of breast reconstruction is essential in order to make improvements in current strategies by identifying variables which affect breast aesthetics [5]. Visual assessment by a panel of observers is the most frequently used method for evaluating patient cosmetic outcome [6]–[8]. The panel may comprise of independent clinicians and lay persons, where each panel member independently scores a range of aspects using photographs of the breasts, taking into account breast symmetry, scars and skin changes [9]. The overall aesthetic outcome of the patient being assessed is scored using a rating scale which ranks comparisons between their treated and untreated breast [10]. Results obtained through panel evaluation have been shown to lack accuracy and reproducibility through low intra and inter-rater agreement [11], [12]. The process is time consuming and impractical as requiring the participation of multiple health professionals is a hindrance when there are large volumes of patients to assess. Effective evaluation of

breast reconstruction surgery requires an objective, consistent and efficient processing technique capable of providing three-dimensional measures of breast aesthetics.

Three-dimensional (3D) imaging has gained credibility in the research environment and has the potential to provide efficient, accurate and repeatable objective outcome measures [13]–[17], incorporating parameters which are not available from two-dimensional images such as volume, surface area, projection, contour and symmetry [10]. Distances between fiducial points on the female torso have been used to objectively quantify aspects of the breast such as ptosis [18]. Current objective breast assessment software BCCT.core [19] and AxisThree [20] require manual placing of landmarks on frontal torso images prior to performing symmetry calculations. Knowledge of surgical terminology is required to accurately locate a number of landmarks on the female torso, therefore these applications require a clinician to carry out the evaluation. The manual landmark procedure is time consuming and has been shown to introduce inter- and intra-observer variability [21]. Automating the detection of fiducial points will achieve efficient, productive, accurate and reliable breast evaluations. This paper investigates a number of algorithms for automated nipple identification on 3D torso surface meshes. Some preliminary results are presented for various thresholding and segmentation techniques by comparing the location of the automatically detected nipple to the manually detected ground truth position. The remainder of this paper is organized as follows. Section 2 highlights work related to this study. Section 3 describes the study methodology including the segmentation approaches assessed and methods of data analysis. Section 4 presents and discusses preliminary results and the study is concluded in Section 5.

2 Related work

Objective outcome measures incorporating algorithms capable of performing automated volumetric, symmetry, shape, scar visibility and projection calculations of the breast region for breast reconstruction would provide clinicians with an efficient, comprehensive and consistent method of evaluation. Implementation of automated detection of prominent points on 3D torso surface images will enable measurements carried out by software to be more usable, efficient and applicable for clinical use. Identifying the location of nipples on a 3D surface mesh will permit symmetry measurements to be performed such as the distance between the left and right nipple, which can be used to objectively assess the cosmetic outcome of a patient. Automatically identifying landmarks on 3D surface images has the potential to enable a patient-friendly method of gathering reliable and accurate anthropometric measurements by reducing intra and inter-observer variability.

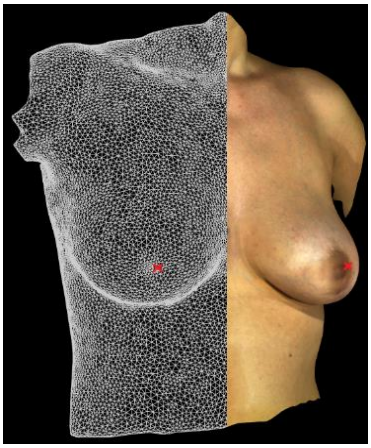

Figure 1: Nipples identified on 3D mesh wireframe and texture.

Merchant *et* al. [22] proposed algorithms to identify the nipples, sternal notch and umbilicus in 3D surface images using surface curvature and 2D texture data. Automatic segmentation of the 3D torso surface image into relative regions of interest regarding the typical location of each anatomical landmark was applied prior to curvature analysis. Gaussian and mean curvature information of the 3D surface enabled landmarks to be detected by searching the 3D image for curvature measurements correlating to the typical features they exhibit. Nipples are commonly located at the peak of the breast mounds, which are convex in shape and exhibit high elliptic Gaussian curvature. To determine an initial estimate for the location of the nipple Merchant *et* al. [22] computed a sum of the Gaussian and mean curvature values and corresponding z-value for each vertex on the 3D surface mesh. The largest value calculated was selected as the initial estimate as nipples are typically regions of high ellipticity and convexity with a high value along the z-axis due to being outwardly projected. 400 vertices surrounding the initial estimate were identified by traversing the mesh and selecting vertices in 1-ring neighborhoods. The colour map of the selected vertices was converted to greyscale before a thresholding operation produced binary pixels. The maximum and minimum intensity values in the greyscale map were retrieved pixels with intensity values less than minimum + 0.1 (maximum – minimum) were

assigned a binary value of 1, and remaining pixels assigned a value of 0. This thresholding procedure permits the selection of points within 10% of the total contrast of the selected sub-region as the nipple areola complex has been found to contain a significantly higher percentage of melanin than the surrounding breast skin making it more pigmented [23]. The centroid of the resulting binarized region can then be computed and mapped back onto the 3D mesh surface, determining the final nipple location [22]. The algorithms were validated by comparing the automatically detected co-ordinates with those manually detected. The study concluded that the landmarks outlined were reliably identified and curvature analysis of 3D surface images is an appropriate technique for determining properties of the breasts such as symmetry and projection which contribute to evaluating breast aesthetics [22].

Detection of nipples on two-dimensional images of female breast was investigated as an approach for adult content recognition by Wang *et* al. [24]. This study opted to use R, G, B colour information in their nipple detection procedure as the nipple skin regularly contains more R (Red) component and less G (Green) component compared to the non-nipple skin which regularly contains less R and more G components. This prior knowledge of colour model composition was used in the two-stage nipple detection algorithm after a canny edge filter was applied. The method proposed by Wang *et* al. [24] was tested on a database of 980 images and the experimental results shown the algorithm to be efficient and accurate when detecting nipples on 2D images of various subject positioning.

Related work has previously focused on implementing automated quantitative analysis of breast morphology in BCCT.core objective software. A semi-automated 2D breast contour detection technique initially developed by Cardoso and Cardoso [25] required manual selection of two breast contour endpoints before the algorithm automatically detected the contour in-between using a shortest path approach. Cardoso *et* al. [26] presented an improved algorithm capable of automatically detecting the endpoints, achieving a fully automatic method of breast contour detection. However the quality of the contour detected was shown to be dependent on position of the subject as the endpoints are located where the contour of the arm intersects the trunk contour and if these are overlapped for instance if the subject places their arms down by their sides then accurate positioning of the endpoints is hindered [26].

3 Methodology

This study investigated modified versions of the approach introduced by Merchant *et* al. [22] for automated detection of the nipples on 3D torso images. In this paper various modified thresholding and additional clustering techniques will be applied to both greyscale and colour 2D texture data of the 3D surface mesh after the initial estimate of the left and right nipple and neighboring vertices have been selected. The position of each automatically identified nipple will be compared to the position of the ground truth, which is manually selected on the 3D torso mesh.

3.1 Experiments

OpenFlipper is an open source, multi-platform application and programming framework which was used for development of algorithms [27].

As the nipples are located at the peak of the breast mound on each breast, the 3D mesh is divided into regions of interest (ROI) in order to perform the search in the area of the mesh where the nipples are likely to be located. Vertices of the mesh are firstly iterated to find the maximum and minimum x and y co-ordinate values on the mesh and using these values the mesh is then split into two halves, left and right each containing one breast. The ROI also takes into account the location of the breasts on the y-axis and focuses on the middle region of the torso. After the ROI's are defined, the vertices in each are searched to find the vertex with the greatest z coordinate which is selected as the initial estimate for the nipple. The uv 2D texture coordinates that are used to map the texture onto the 3D mesh are retrieved for neighboring vertices of the initial estimate and used to calculate the x and y position of each selected vertex on the 2D texture image using Equations (1) and (2).

$$x = u * texture\_width \tag{1}$$

$$y = texture\_height - (v * texture\_height) \tag{2}$$

Various thresholding and clustering techniques are then applied to both greyscale and colour 2D texture data of the selected vertices on the 3D surface mesh in effort to segment the nipple from the surrounding areola and skin. The centroid of the segmented region or cluster is computed as an x, y location on the 2D texture, which is then remapped onto the 3D mesh and selected as the final nipple location.

The following sections will describe in detail the procedure used in each experiment to segment the nipple from surrounding skin using 2D texture data to locate the position of the nipple on the 3D surface mesh.

3.1.1 10% thresholding

Thresholding is an approach used to segment an image by taking a greyscale image as input and setting pixels with intensity values higher than a threshold to 0 and all remaining pixels to 1; producing a binary image. This approach to thresholding used in the study by Merchant *et* al. [22] allows the selection of points that are within 10% of the total contrast of the sub-region containing neighboring vertices of the initial nipple estimate. The image texture file belonging to the 3D mesh currently loaded is retrieved by the software and converted to greyscale. The pixel intensity values of selected vertices are searched to find the maximum and minimum. These values are then used in Equations (3) and (4) to calculate a threshold value.

$$threshold\_left = min\_left + 0.1\ (max\_left - min\_left) \quad (3)$$

$$threshold\_right = min\_right + 0.1\ (max\_right - min\_right) \quad (4)$$

Pixels less than the threshold value are assigned a value of 1 and the remaining pixels a value of 0. The centroid of the pixels assigned a value of 1 is then calculated and remapped onto the 3D mesh as the final nipple location.

3.1.2 20% thresholding

The thresholding applied here follows the same approach as above, however allows the selection of points within 20% of the total intensity of the sub-region. The pixel intensity values of selected vertices are searched to find the maximum and minimum. These values are then used in Equations (5) and (6) to calculate a threshold value.

$$threshold\_left = min\_left + 0.2\ (max\_left - min\_left) \quad (5)$$

$$threshold\_right = min\_right + 0.2\ (max\_right - min\_right) \quad (6)$$

Once again pixels less than the threshold value are assigned a value of 1 and the remaining pixels a value of 0 and the centroid of the pixels assigned a value of 1 position is determined before being remapped back onto the 3D mesh.

3.1.3 Otsu automated thresholding

Rather than simply setting a threshold based on pixels with intensities within a certain percentage of the total contrast as above an automated approach to thresholding can be used. Otsu's automated thresholding method assumes that the extracted texture data of the selected sub-region of neighboring vertices contains two classes of pixels, the nipple and surrounding areola. The image data is first converted to greyscale and a histogram is created of the pixel intensities. The optimum threshold of the bimodal histogram is calculated by Otsu and the pixel intensities of selected vertices are checked. If the intensity is less than the optimum threshold the pixel is assigned a value of 1 and if the intensity is greater a value of 0. The centroid is located and remapped back onto the mesh as before.

3.1.4 K-Means clustering RGB colour model

K-Means clustering is one of the simplest unsupervised learning algorithms [28]. Image segmentation using k-means assigns labels to each pixel in the 2D image texture based on their RGB colour values. Pixels of similar colour formation are assigned the same label and therefore belong to the same cluster. With reference to our data it is hoped that pixels belonging to the nipple will belong to a different cluster than pixels from the surrounding nipple areola complex. The image texture file belonging to the 3D mesh currently loaded is retrieved by the software and mapped into samples, each dataset of the sample consists of a RGB pixel group. The number of clusters required has been empirically selected as 5 to permit adequate segmentation of the nipple from surrounding areola and skin. K-Means is then executed on the texture image and the centers of the computed clusters mapped onto a clustered image as shown in Figure 2. The texture location of the initial nipple estimate's neighboring vertices on the clustered image is accessed and the smallest cluster determined. The centroid of the smallest cluster is remapped onto the mesh as the final nipple position.

Figure 2: Clustered RGB image.

3.1.5 K-Means clustering HSV colour model

K-means clustering is carried out using the HSV colour space for this experiment. The HSV colour space is often preferred over the RGB colour model in image segmentation as it separates colour information and intensity [29]. The image texture file is converted into the HSV colour space and mapped into samples, each dataset of the sample consists of a HSV pixel group. The number of clusters required has been empirically selected as 5 to permit adequate segmentation of the nipple from surrounding areola and skin. K-Means is then executed on the texture image and the centers of the computed clusters mapped to onto a clustered image. Once again the smallest cluster in the sub-region is determined and it's centroid of the smallest cluster is remapped onto the mesh as the final nipple position.

3.2 Data analysis

The methodology proposed in this paper for this initial study was assessed on a dataset of four 3D frontal torso surface meshes to gather preliminary results. The performance of each experiment was evaluated by comparing the 3D coordinates of the automatically detected nipples and the manual placement of each nipple in the software, which was used as the ground truth. To compare the position of the nipples located automatically and manually, the euclidean distance (mm) between the automatically detected coordinates and those manually marked on software was calculated using Equation (7)

$$distance = \sqrt{(x_2 - x_1)^2 + (y_2 - y_1)^2 + (z_2 - z_1)^2} \tag{7}$$

where x_1, y_1, z_1 are the vertex coordinates of the automatically detected nipple and x_2, y_2, z_2 are the vertex coordinates of the manually located nipple.

The ground truth nipple position was determined for each mesh by manually marking the left and right nipple on the surface mesh. The vertex position of each manually located nipple is then stored to be used as in each experiment to calculate the distance between the ground truth and the automated position of each nipple.

4 Preliminary results and discussion

Left and right nipples were automatically detected on four 3D surface meshes by performing the procedures outlined in Section 3. The euclidean distance (mm) between the automatically detected nipple and the manual ground truth was determined for each procedure. The distances calculated for each of the 4 meshes and average for each approach are presented in Table 1.

Table 1: Distances (mm) between the automated and ground truth positions for the left (NL) and right nipple (NR)

Approach	Mesh #1		Mesh #2		Mesh #3		Mesh #4		Average of 4 Meshes (mm)	
	NL	NR	NL	NR	NL	NR	NL	NR	NL	NR
10% threshold	4.84	4.79	6.68	0.00	7.07	5.00	6.38	3.17	6.24	3.24
20% threshold	2.28	5.80	4.63	0.00	7.07	2.91	2.68	2.87	4.16	2.90
K-Means (RGB)	2.28	4.79	4.63	0.00	7.07	2.91	2.68	0.00	4.16	1.92
K-Means (HSV)	4.84	3.88	18.40	12.30	25.62	21.54	5.59	2.87	13.61	10.15
Otsu threshold	4.84	23.51	15.76	0.00	25.87	2.91	26.62	24.75	18.27	12.79

The initial results for K-Means (RGB) clustering were promising with the algorithm performing more accurate nipple detection than the 10% thresholding method initially proposed by Merchant *et* al. [22] on five out of the total eight occasions and matching the accuracy of 10% thresholding on the remaining three. Position of the automatically detected right nipple for Mesh #2 and #4 (Figure 3(c)) equaled the manual ground truth position using the K-Means (RGB) approach, where the 10% thresholding algorithm resulted in less accurate detection of the right nipple for Mesh #4. The proposed K-Means (RGB) clustering approach may have produced more accurate preliminary results than the method suggested by Merchant *et* al. [22] because of the extra information at pixel level contained in the RGB colour model compared to the greyscale image data used in the 10% thresholding algorithm. The 20% thresholding results were encouraging for the left nipple, however didn't match the accuracy of the K-Means (RGB) clustering method for detecting the right nipple which produced the lowest average of 1.92mm. K-Means (HSV) performed well on Mesh #1 and #4, generating lower euclidean distances than the 10% thresholding approach on 4 occasions, however poor performance on Mesh #2 and #3 resulted in a high average. The Otsu automated thresholding approach proved to be the least accurate at detecting both nipples for all meshes in our initial dataset. This may due to Otsu's method of thresholding relying on bimodal histogram to select an optimum threshold between two peaks representing the foreground and background, which may not have been the case for the texture image data of the initial dataset [30]. Variation between distances calculated for the left and right nipple was present in all 4 meshes, this may have been caused by changes in lighting conditions over the torso region impairing the quality of the texture image. The variation in lighting conditions of surface meshes is to be expected therefore further development of algorithms should aim to perform accurate nipple detection taking this into consideration.

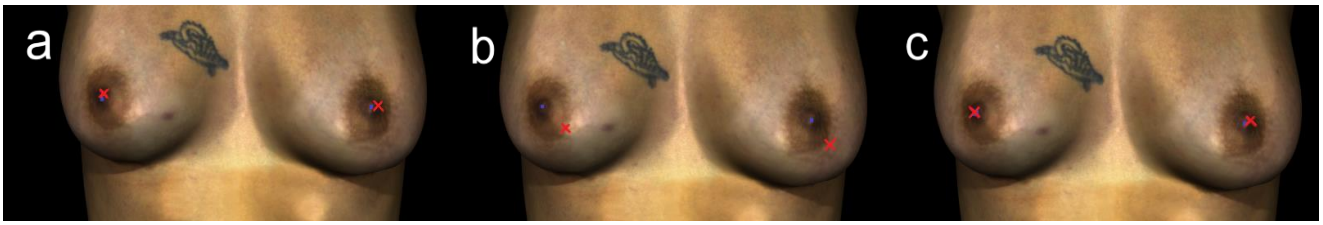

Figure 3: Automatically detected nipples (red cross) and manual ground truth (blue square) after executing (a) 10% thresholding (b) Otsu (c) K-Means (RGB) on Mesh #4.

5 Conclusion

This paper presents various segmentation techniques using both greyscale and colour image data combined with 3D surface meshes to distinguish the nipple from surrounding areola and skin on 3D torso surface images. Segmentation using colour information from the 2D texture data of the 3D mesh presented promising initial results with K-Means (RGB) performing the most accurate detection on average for the right nipple when compared to the other approaches, however as this study was carried out using a small initial dataset the robustness of all algorithms could not be assessed completely. There is clear potential for the 20% thresholding which matched the accuracy of the K-Means (RGB) algorithm when detecting the left nipple, with both approaches obtaining the lowest average. The K-Means (HSV) clustering method produced very good results for some meshes proving to be more accurate than Otsu automated thresholding method. Future work will focus on improving segmentation algorithms by performing clustering on the sub-region of the initial estimate instead of the entire texture and ensuring algorithms are able to perform accurate nipple detection on meshes with varying lighting conditions.

References

[1] Northern Ireland Cancer Registry (NICR), "Breast cancer," 2013. [Online]. Available: http://www.qub.ac.uk/research-centres/nicr/FileStore/PDF/FactSheets/Filetoupload,629853,en.pdf. [Accessed: 22-Mar-2016].

[2] Cancer Research UK, "Breast Cancer Mortality." [Online]. Available: http://www.cancerresearchuk.org/health-professional/cancer-statistics/statistics-by-cancer-type/breast-cancer#heading-Two. [Accessed: 01-Nov-2015].

[3] D. A. Hudson, "Factors determining shape and symmetry in immediate breast reconstruction.," *Ann. Plast. Surg.*, vol. 52, no. 1, pp. 15–21, Jan. 2004.

[4] J. Sabczynski, H. Barschdorf, T. Bülow, M. J. Cardoso, J. S. Cardoso, A. Clarke, B. Eiben, P. Gouveia, D. Hawkes, J. Hipwell, M. Keshtgar, R. Lacher, D. Kutra, G.-J. Liefers, K. Meetz, B. Molenkamp, J. P. Monteiro, A. Mosahebi, H. P. Oliveira, R. Sinkus, D. Stoyanov, V. Vavourakis, C. Jh Van De Velde, N. Williams, S. Young, and H. Zolfagharnasab, "PICTURE: Predicting the cosmetic outcome of breast cancer surgery."

[5] M. J. Cardoso, H. Oliveira, and J. Cardoso, "Assessing cosmetic results after breast conserving surgery.," *J. Surg. Oncol.*, vol. 110, no. 1, pp. 37–44, 2014.

[6] D. R. H. Christie, M. Y. O'Brien, J. A. Christie, T. Kron, S. A. Ferguson, C. S. Hamilton, and J. W. Denham, "A comparison of methods of cosmetic assessment in breast conservation treatment," *The Breast*, vol. 5, no. 5, pp. 358–367, Oct. 1996.

[7] K. C. A. Sneeuw, N. K. Aaronson, J. R. Yarnold, M. Broderick, J. Regan, G. Ross, and A. Goddard, "Cosmetic and functional outcomes of breast conserving treatment for early stage breast cancer. 1. Comparison of patients' ratings, observers' ratings and objective assessments," *Radiother. Oncol.*, vol. 25, no. 3, pp. 153–159, Nov. 1992.

[8] C. Vrieling, L. Collette, E. Bartelink, J. H. Borger, S. J. Brenninkmeyer, J. C. Horiot, M. Pierart, P. M. Poortmans, H. Struikmans, E. Van Der Schueren, J. a. Van Dongen, E. Van Limbergen, and H. Bartelink, "Validation of the methods of cosmetic assessment after breast-conserving therapy in the EORTC 'boost versus no boost' trial," *Int. J. Radiat. Oncol. Biol. Phys.*, vol. 45, no. 3, pp. 667–676, 1999.

[9] M. H. Haloua, N. M. A. Krekel, G. J. A. Jacobs, B. Zonderhuis, M. Bouman, M. E. Buncamper, F. B. Niessen, H. A. H. Winters, C. Terwee, S. Meijer, and M. P. van den Tol, "Cosmetic Outcome Assessment following Breast-Conserving Therapy: A Comparison between BCCT.core Software and Panel Evaluation," *Int. J. Breast Cancer*, vol. 2014, pp. 1–7, 2014.

[10] M. S. Kim, J. C. Sbalchiero, G. P. Reece, M. J. Miller, E. K. Beahm, and M. K. Markey, "Assessment of breast aesthetics.," *Plast. Reconstr. Surg.*, vol. 121, no. 4, p. 186e–94e, 2008.

[11] M. J. Cardoso, J. Cardoso, A. C. Santos, H. Barros, and M. C. de Oliveira, "Interobserver agreement and consensus over the esthetic evaluation of conservative treatment for breast cancer," *The Breast*, vol. 15, no. 1, pp. 52–57, 2006.

[12] H. Henseler, J. Smith, A. Bowman, B. S. Khambay, X. Ju, A. Ayoub, and A. K. Ray, "Subjective versus objective assessment of breast reconstruction," *J. Plast. Reconstr. Aesthetic Surg.*, vol. 66, no. 5, pp. 634–639, 2013.

[13] K. Aldridge, S. A. Boyadjiev, G. T. Capone, V. B. DeLeon, and J. T. Richtsmeier, "Precision and error of three-dimensional phenotypic measures acquired from 3dMD photogrammetric images," *Am. J. Med. Genet. Part A*, vol. 138A, no. 3, pp. 247–253, 2005.

[14] T. Catherwood, E. McCaughan, E. Greer, R. A. J. Spence, S. A. McIntosh, and R. J. Winder, "Validation of a passive stereophotogrammetry system for imaging of the breast: A geometric analysis," *Med. Eng. Phys.*, vol. 33, no. 8, pp. 900–905, 2011.

[15] D. L. Esme, A. Bucksch, and W. H. Beekman, “Three-Dimensional Laser Imaging as a Valuable Tool for Specifying Changes in Breast Shape After Augmentation Mammaplasty,” *Aesthetic Plast. Surg.*, vol. 33, no. 2, pp. 191–195, 2009.
[16] H. Henseler, J. Smith, A. Bowman, B. S. Khambay, X. Ju, A. Ayoub, and A. K. Ray, “Investigation into variation and errors of a three-dimensional breast imaging system using multiple stereo cameras,” *J. Plast. Reconstr. Aesthetic Surg.*, vol. 65, no. 12, pp. e332–e337, 2012.
[17] L. Kovacs, M. Eder, R. Hollweck, A. Zimmermann, M. Settles, A. Schneider, M. Endlich, A. Mueller, K. Schwenzer-Zimmerer, N. a. Papadopulos, and E. Biemer, “Comparison between breast volume measurement using 3D surface imaging and classical techniques,” *Breast*, vol. 16, no. 2, pp. 137–145, 2007.
[18] M. S. Kim, G. P. Reece, E. K. Beahm, M. J. Miller, E. Neely Atkinson, and M. K. Markey, “Objective assessment of aesthetic outcomes of breast cancer treatment: Measuring ptosis from clinical photographs,” *Comput. Biol. Med.*, vol. 37, no. 1, pp. 49–59, 2007.
[19] M. J. Cardoso, J. Cardoso, N. Amaral, I. Azevedo, L. Barreau, M. Bernardo, D. Christie, S. Costa, F. Fitzal, J. L. Fougo, J. Johansen, D. Macmillan, M. P. Mano, L. Regolo, J. Rosa, L. Teixeira, and C. Vrieling, “Turning subjective into objective: The BCCT.core software for evaluation of cosmetic results in breast cancer conservative treatment,” *The Breast*, vol. 16, no. 5, pp. 456–461, 2007.
[20] “Axis Three for Breast Simulations,” 2016. [Online]. Available: http://www.axisthree.com/products/breast-surgery-simulation. [Accessed: 24-May-2016].
[21] M. Kawale, J. Lee, S. Y. Leung, M. C. Fingeret, G. P. Reece, M. A. Crosby, E. K. Beahm, M. K. Markey, and F. A. Merchant, “3D Symmetry measure invariant to subject pose during image acquisition,” *Breast Cancer Basic Clin. Res.*, vol. 5, no. 1, pp. 131–142, 2011.
[22] F. Merchant, M. Kawale, G. Reece, M. Crosby, E. Beahm, M. Fingeret, and M. Markey, “Automated Identification of Fiducial Points on 3D Torso Images,” *Biomed. Eng. Comput. Biol.*, p. 57, 2013.
[23] N. Dean, J. Haynes, J. Brennan, T. Neild, C. Goddard, B. Dearman, and R. Cooter, “Nipple-areolar pigmentation: Histology and potential for reconstitution in breast reconstruction,” *Br. J. Plast. Surg.*, vol. 58, no. 2, pp. 202–208, 2005.
[24] Y. Wang, J. Li, H. Wang, and Z. Hou, “Automatic nipple detection using shape and statistical skin color information,” *Lect. Notes Comput. Sci. (including Subser. Lect. Notes Artif. Intell. Lect. Notes Bioinformatics)*, vol. 5916 LNCS, pp. 644–649, 2009.
[25] J. S. Cardoso and M. J. Cardoso, “Breast contour detection for the aesthetic evaluation of breast cancer conservative treatment,” *Adv. Soft Comput.*, vol. 45, pp. 518–525, 2007.
[26] J. S. Cardoso and L. F. Teixeira, “Automatic breast contour detection in digital photographs,” *Int. Conf. Heal. Informatics*, pp. 91–98, 2008.
[27] “OpenFlipper,” 2016. [Online]. Available: www.openflipper.org. [Accessed: 24-May-2016].
[28] A. Mohanty, “Analysis of Color Images using Cluster based Segmentation Techniques,” vol. 79, no. 2, pp. 42–47, 2013.
[29] S. Sural, G. Qian, and S. Pramanik, “Segmentation and histogram generation using the HSV color space for image retrieval,” *Int. Conf. Image Process.*, vol. 2, pp. II–589–II–592, 2002.
[30] N. Otsu, “A threshold selection method from gray-level histograms,” *IEEE Trans. Syst. Man. Cybern.*, vol. 9, no. 1, pp. 62–66, 1979.